Methods 77–78 (2015) 92–103

Contents lists available at ScienceDirect

Methods

journal homepage: www.elsevier.com/locate/ymeth

Study of PTEN subcellular localization

Angela Bononi [1], Paolo Pinton *

Section of Pathology, Oncology and Experimental Biology, Laboratory for Technologies of Advanced Therapies (LTTA), Department of Morphology, Surgery and Experimental Medicine, University of Ferrara, Ferrara, Italy

ARTICLE INFO

Article history:
Received 31 July 2014
Received in revised form 28 September 2014
Accepted 2 October 2014
Available online 13 October 2014

Keywords:
Mitochondria
Endoplasmic reticulum
Cancer
Calcium
Cell death
Apoptosis

ABSTRACT

The tumor suppressor PTEN is a key regulator of a plethora of cellular processes that are crucial in cancer development. Through its lipid phosphatase activity PTEN suppresses the PI3K/AKT pathway to govern cell proliferation, growth, migration, energy metabolism and death. The repertoire of roles fulfilled by PTEN has recently been expanded to include crucial functions in the nucleus, where it favors genomic stability and restrains cell cycle progression, as well as protein phosphatase dependent activity at the endoplasmic reticulum (ER) and mitochondria-associated membranes (MAMs), where PTEN interacts with the inositol 1,4,5-trisphosphate receptors (IP3Rs) and regulates Ca^{2+} release from the ER and sensitivity to apoptosis. Indeed, PTEN is present in definite subcellular locations where it performs distinct functions acting on specific effectors. In this review, we summarize recent advantages in methods to study PTEN subcellular localization and the distinct biological functions of PTEN in different cellular compartments. A deeper understanding of PTEN's compartmentalized-functions will guide the rational design of novel therapies.

1. Introduction

Following the discovery of phosphatase and tensin homolog deleted on chromosome 10 (PTEN) numerous efforts have identified its pleiotropic functions not only in various processes central to cancer development, but also in a wide range of biological functions beyond tumor suppression. PTEN is a non-redundant, evolutionarily-conserved, dual-specificity phosphatase capable of removing phosphates from protein [1] and lipid substrates [2]. PTEN has long been known as a lipid phosphatase that catalyzes the conversion of phosphatidylinositol-3,4,5-trisphosphate (PIP3) to phosphatidylinositol-4,5-bisphosphate (PIP2). Loss of PTEN function leads to excessive PIP3 accumulation at the plasma membrane and subsequent derepression of the PI3K/AKT pathway, which in turn stimulates cell growth, proliferation, survival, and other cellular processes [3,4].

PTEN mutations occur frequently in tumors and in the germline of patients predisposed to tumor development, or cognitive and metabolic disorders [5,6]. PTEN is also essential for embryonic development, as homozygous PTEN deletion results in developmental defects and embryonic lethality [7]. The wide array of functions mediated by PTEN in controlling diverse fundamental physiological and pathological processes is tightly governed by multiple regulatory mechanisms.

PTEN expression and activity is regulated at almost all levels: transcriptional, translational and post-translational. Post-translational modifications, including phosphorylation, oxidation, acetylation, S-nitrosylation, ubiquitination, sumoylation, and interactions with other proteins are perhaps the most important mechanisms of PTEN regulation [8]. As post-translational modifications and

Abbreviations: AKAP, A kinase anchoring protein; ArA, arachidonic acid; Ca^{2+}, calcium; CLS, cytoplasmic localization signal; Co-IP, co-immunoprecipitation; COX, cytochrome *c* oxidase; ER, endoplasmic reticulum; ER-RFP, endoplasmic reticulum-targeted red fluorescent protein; FRAP, fluorescence recovery after photobleaching; GFP, green fluorescent protein; HAUSP, herpesvirus-associated ubiquitin-specific protease; HK-I, hexokinase I; IF, immunofluorescence; IP3R, inositol 1,4,5-trisphosphate receptor; IPC, ischemic preconditioning; I/R, ischemia–reperfusion; MAMs, mitochondria-associated membranes; mtDsRED, mitochondria-targeted red fluorescent protein; Ndfip1, NEDD4 family-interacting protein 1; NEDD4, neural precursor cell expressed developmentally downregulated-4; NES, nuclear export signal; NLS, nuclear localization signal; OMM, outer mitochondrial membrane; PAM, plasma membrane–associated membranes; PIP2, phosphatidylinositol-4,5-bisphosphate; PIP3, phosphatidylinositol-3,4,5-trisphosphate; PK, proteinase K; PM, plasma membrane; PML, promyelocytic leukemia; PTEN, phosphatase and tensin homolog deleted on chromosome 10; RFP, red fluorescent protein; ROS, reactive oxygen species; STS, staurosporine; YFP, yellow fluorescent protein; VDAC, voltage-dependent anion channel.

* Corresponding author at: Section of Pathology, Oncology and Experimental Biology, Department of Morphology, Surgery and Experimental Medicine, University of Ferrara, Via Fossato di Mortara 70 (c/o CUBO), 44121 Ferrara, Italy.
E-mail address: pnp@unife.it (P. Pinton).
[1] Present address: University of Hawaii Cancer Center, University of Hawaii, Honolulu, HI, USA.

http://dx.doi.org/10.1016/j.ymeth.2014.10.002
1046-2023/

binding partners influence the association of PTEN to the plasma membrane and other cellular compartments, they play a crucial role in the regulation of PTEN functions. A better understanding of these mechanisms is critical because a significant body of evidence suggests that PTEN also has PI3K/AKT-independent activities and can localize to specific cellular compartments, where it exerts specific tumor suppressive functions.

Early studies proposed that PTEN localizes exclusively to the cytoplasm and was able to transiently associate with the plasma membrane depending on the local phosphatidylinositol-4,5-bisphosphate (PIP2) and PIP3 concentrations [9,10]. However, PTEN has recently been shown to localize to or associate with organelles and specialized subcellular compartments, such as the nucleus and the nucleolus, the mitochondria, the endoplasmic reticulum (ER) and the mitochondria-associated membranes (MAMs) [11–15]. Finally, PTEN can be secreted/exported into the extracellular environment for uptake by recipient cells, within which it functions as an intercellular tumor suppressor [16,17].

1.1. Plasma membrane PTEN

Binding to the plasma membrane is a critical regulatory step for PTEN function in antagonizing the PI3K signaling pathway. However, in most mammalian cell types, PTEN does not show an obvious association with the plasma membrane. Instead, PTEN is mainly found in the cytosol and nucleus. PTEN possesses an N-terminal PIP2-binding motif, a C2 domain, and a C-terminal tail that are involved in its membrane targeting. The N-terminal domain of PTEN can bind specifically to PIP2, therefore local PIP2 and PIP3 gradients influence the membrane binding and activation of PTEN [18,19]. The crystal structure of PTEN also revealed a C2 domain that harbors basic residues essential for membrane binding [20]. In addition, the C-terminal, apparently unstructured and flexible tail of PTEN, contains a cluster of serine and threonine phosphorylation sites (S370, S380, T382, T383, and S385) that regulate its stability, activity, and recruitment to the cell membrane. Multiple kinases are capable of phosphorylating the C-terminal tail of PTEN. Vazquez et al. have proposed that phosphorylated PTEN assumes a closed conformation (due to interaction between the phosphorylation cluster of the C-terminal tail and the positively charged surface on the C2 domain) that opposes membrane binding and keeps PTEN inactive in the cytoplasm [21,22]. More recently also SUMO1 modification of PTEN has been shown to regulate its association with the plasma membrane, and in particular SUMOylation occurring at K^{266} seems essential for its tumor-suppressor function [23].

1.2. Nuclear PTEN

In the nucleus, PTEN has important tumor-suppressive functions. The absence of nuclear PTEN is associated with more aggressive cancers, making nuclear PTEN a useful prognostic indicator in some cancer types [24]. Given the absence of a classical nuclear localization signal, the mechanism of PTEN nuclear localization has yet to be fully elucidated. Numerous molecular mechanisms have been proposed, including simple diffusion [25] and active shuttling regulated by a putative nuclear localization signal (NLS) that mediate PTEN interaction with the major vault protein [26]. PTEN also has a cytoplasmic localization signal (CLS) in the N-terminal region (amino acids 19–25) required for cytoplasmic localization that could acts as a non-canonical signal for nuclear export [27]. Also interaction with the GTPase Ran has been proposed to control PTEN nuclear/cytoplasmic accumulation based on the existence of multiple nuclear exclusion motifs at distinct PTEN regions, and a nuclear localization domain at the PTEN N-terminus [28]. The authors showed that a chimera containing the first 32 residues of PTEN fused with GST-green fluorescent protein (GFP) (PTEN 1–32/GSTGFP) has intense nuclear accumulation, and proposed that changes in the conformation of PTEN following receipt of apoptotic or cell growth inhibitory signals would unmask the N-terminal nuclear localization domain and trigger PTEN nuclear entry by a Ran-dependent mechanism. Nevertheless, the mechanisms of PTEN nucleus-cytoplasmic shuttling appear to involve also posttranslational modifications such as monoubiquitination or sumorylation. NEDD4-1 (neural precursor cell expressed, developmentally downregulated-4-1)-mediated monoubiquitination promote PTEN nuclear import [11] while herpesvirus-associated ubiquitin-specific protease (HAUSP)-mediated PTEN deubiquitination trigger nuclear exclusion [29]. Recently also sumoylation-mediated PTEN nuclear retention has been reported [12].

Nuclear PTEN maintains chromosomal stability by interacting with the centromere proteins centromere protein-C (CENP-C) [30], and participates in DNA-damage responses by up-regulating the transcription of Rad51 that leads to double-strand break repair [30]. In addition, nuclear PTEN controls cell-cycle progression by inducing G0–G1 arrest most likely as a result of cyclin D1 downregulation [31], and regulates cellular senescence through anaphase promoting complex (APC)-CDH1-mediated protein degradation [32].

Cerebral ischemia was reported as the first physiological mechanism able to dynamically alter the subcellular localization of PTEN *in vivo* [33]. In this study, PTEN ubiquitination and translocation from the cytoplasm to the nucleus were shown to occur after cerebral ischemia in the brain, leading unexpectedly to neuron survival.

PTEN also localizes to the nucleolus, where it regulates nucleolar homeostasis and morphology [13]. Most of these functions of nuclear PTEN are independent of its phosphatase activity and unrelated to the PI3K/AKT pathway. Indeed, although nuclear pools of PIP3 have been reported, they belong to distinct, partially detergent-resistant proteolipid complexes that are not dynamically regulated and are therefore not likely PTEN substrates [34], suggesting a potential role for nuclear PTEN beyond its lipid phosphatase activity.

1.3. PTEN at the mitochondria, ER and MAMs

Recently, several lines of evidence noted the ability of PTEN to also interact with intracellular membrane-containing organelles. This unique feature of PTEN was initially revealed by fluorescence recovery after photobleaching (FRAP) studies showing that that nuclear PTEN diffused very rapidly and appeared not to be tethered, while cytoplasmic PTEN diffused more slowly suggesting transient interactions with immobile cytoplasmic structures [25]. Therefore, it was important to understand if this tethering of PTEN to cytoplasmic structures prevents it from acting at the plasma membrane, or if it localizes PTEN to specific subcellular domains where it acts as a tumor suppressor through other mechanisms.

PTEN localization to the mitochondria surface has been demonstrated both by immunocytochemistry and biochemical fractionation experiments: (i) in primary rat hippocampal neurons after apoptotic stimulation using staurosporine (STS), (ii) in myocytes during myocardial ischemia–reperfusion (I/R) and (iii) in cell lines [14,15,35]. Mitochondria-localized PTEN sustains ROS production and contributes to mitochondria-dependent apoptosis.

Liang et al. identified an N-terminally extended form of PTEN (named PTENα) that localizes to the cytoplasm and the mitochondria [36]. The authors not only demonstrated that this longer form of PTEN is necessary for the maintenance of mitochondrial structure and function, potentially by maintaining cytochrome *c* oxidase (COX) in a hypo-phosphorylated state, but also suggested that it

collaborates with canonical PTEN in regulating mitochondrial energy metabolism.

Immunostaining and subcellular fractionation experiments carried out in our laboratory also revealed that a fraction of PTEN localizes to the ER and MAMs [15]. Here, PTEN regulates calcium (Ca^{2+}) release from the ER, subsequent Ca^{2+} accumulation in the mitochondria and sensitivity to apoptosis [37–39]. Co-immunoprecipitation experiments showed that PTEN interacts with the inositol-1,4,5-trisphosphate receptors (IP3Rs), and counteracts the reduced IP3R3–Ca^{2+} release mediated by AKT phosphorylation of the receptor [40–43], in a protein phosphatase-dependent manner. PTEN localization to the ER appears to be part of the Ca^{2+}-mediated apoptotic process, as both fractionation and live in vitro imaging colocalization experiments demonstrate a further accumulation of PTEN at the ER during Ca^{2+}-mediated apoptotic induction [15,44].

1.4. Extracellular PTEN

Recently two different groups have reported that PTEN is also secreted/exported outside the cell. Putz et al. [16] demonstrated that PTEN is exported in exosomes under the control of NEDD4 family-interacting protein 1 (Ndfip1), an adaptor protein for the NEDD4 ubiquitin ligase; extracellular PTEN is then internalized by recipient cells and is able to reduce AKT phosphorylation and cell proliferation. Hopkins et al. [17] identified a previously uncharacterized form of PTEN containing an additional 173 amino acids at the N-terminal of the 403-amino acid-long WT PTEN protein (named PTEN-Long), which resulted from an alternate translation initiation site. This longer form of PTEN is a membrane-permeable lipid phosphatase that is secreted from cells, and is capable of entering other cells where it antagonizes the PI3K signaling pathway.

In order to unify nomenclature and amino acid numbering, the longer form of PTEN, initially named PTEN-Long [17] or PTENα [36], has recently been renamed PTEN-L [45].

These findings expand the current understanding of PTEN functions in the control of diverse fundamental biological processes, which cannot be attributed merely to its phosphatase activity and regulation of the PI3K/AKT pathway. Indeed, in addition to mutation or deletion of the PTEN gene, other pathological mechanisms that result in the aberrant subcellular compartmentalization of the PTEN protein are associated with cancer. A further investigation of the mechanisms underlying PTEN subcellular localization may provide a foundation for the development of novel therapies targeting PTEN.

It is generally accepted that the subcellular localization of a protein is tied to its functions, and this has been widely proven, especially in the case of PTEN. Therefore, it is important to be able to determine where PTEN resides and how its exact function relates to a specific subcellular localization. In the following paragraphs, we will describe different methods that have been used to highlight PTEN trafficking and subcellular localization.

2. Subcellular fractionation methods

Back in 2001, Leslie et al. showed that in U87MG cells fractionated to give membrane and soluble proteins, only a small fraction of PTEN was associated with the plasma membrane; however, the functional significance of this was unclear [46]. A remarkable number of studies that followed not only validated this puzzling observation, but also showed that dynamic membrane associations could be modulated temporally or spatially to alter PTEN activity, and demonstrated the functional role of PTEN in many other cellular compartments.

The first subcellular fractionation data that detected PTEN in the nucleus came from a study of PTEN's role in neuronal differentiation [47]. Nuclear and cytosolic fractions were prepared from PC12 cells and CNS stem cells as described in [48]. Nuclear/cytoplasmic fractionation of PTEN after ubiquitin overexpression was used to demonstrate the role of PTEN monoubiquitination in its nuclear import; moreover because nuclear PTEN was not quantitatively monoubiquitinated, the authors suggested that only deubiquitinated PTEN remained nuclear, whereas its ubiquitinated form was re-exported [11]. Subsequently, the promyelocytic leukemia (PML) tumor suppressor was found to regulate PTEN compartmentalization, by inhibiting HAUSP-mediated deubiquitinylation [29]. The authors performed a nuclear and cytoplasmic fractionation of PTEN after treating NB4 or all-*trans* retinoic acid (ATRA)-resistant NB4 cells with arsenic trioxide (ATO) or ATRA, agents that induce degradation of the PML-Retinoic Acid Receptor-Alpha (RARα) oncoprotein and restores PML nuclear bodies. Specifically, 4 h of ATO treatment reconstituted PML nuclear bodies and restored PTEN localization to the nucleus, whereas 24 h of treatment abolished the nuclear bodies along with a concomitant localization of PTEN to the cytoplasm.

In a recent study, PTEN was also found to be localized to the nucleolus [13]. A fractionation protocol modified from Busch et al. [49] was used to isolate nucleoli from HeLa cells, and western blot analysis showed enriched levels of PTEN protein in nucleoli, compared to that in total cell lysates.

PTEN accumulation in the mitochondria was originally observed in mitochondria isolated from primary rat hippocampal neurons undergoing apoptosis [14]. A time-dependent accumulation of PTEN in the mitochondria and immunoprecipitation with Bax was detected after STS treatment, suggesting the involvement of PTEN in the regulation of mitochondria-dependent apoptosis. The mitochondrial localization of PTEN and association with Bax was later confirmed in isolated mouse hearts exposed to ischemia and reperfusion (I/R) [35]. The biological functions of PTEN in the subcellular space had never been studied before in the heart. Heart fractionations showed that mitochondrial PTEN and Bax protein levels, as well as the physical association between them, were increased by I/R and attenuated by ischemic preconditioning (IPC). The authors also found that in reperfused hearts, ROS promotes the mitochondrial localization of PTEN. Indeed, in hearts perfused with the ROS scavenger, N-acetylcysteine, mitochondrial PTEN protein levels were decreased. Reciprocally, treatment with H_2O_2 to mimic I/R-induced ROS increased mitochondrial PTEN protein levels.

Various protocols are available to isolate mitochondria [50], but these are mostly limited to the isolation of a "relatively pure", or "crude", mitochondria fraction. This "crude" mitochondria fraction almost always contains contaminations from other compartments, in particular the ER, MAMs, nucleus and cytoplasm. To definitively characterize the localization of PTEN under basal conditions and in cells undergoing apoptosis, we utilized a cell fractionation protocol that we had previously established. This comprehensive procedure is described in detail in [51]. A summary of the reagents is provided in Table 1 and a snapshot protocol is displayed in Fig. 1. This protocol allows the isolation of a pure mitochondria fraction, wherein the ER, the nuclear and other non-mitochondrial markers become undetectable; moreover, it permits the isolation of the ER, as well as the MAMs fraction that contains unique regions of ER membranes attached to the outer mitochondrial membrane (OMM). We isolated these fractions from cultured cells (HEK-293 or MEF) and demonstrated that in addition to the cytosol, PTEN is also localized to the mitochondria, ER and MAMs fractions [15].

To further discriminate whether PTEN associates with the OMM or resides within these organelles, purified mitochondria were treated with proteinase K (PK), which can only digest those

Table 1
Setup of subcellular fractionation stock solutions and buffers. Catalog numbers of the reagents are provided at the bottom of the table.

Subcellular fractionation stock solutions and buffers *Setup*	
0.5 M EGTA (pH 7.4)	In 70 ml of bi-distilled water, dissolve: **19 g** of **EGTA** adjust **pH** to **7.4** with *KOH*, bring the solution to **100 ml** with bi-distilled water, Store at 4 °C
0.5 M HEPES (pH 7.4)	In 400 ml of bi-distilled water, dissolve: **59.57 g** of **HEPES** adjust **pH** to **7.4** using *KOH*, bring the solution to **500 ml** with bi-distilled water, Store at 4 °C
1 M Tris–HCl (pH 7.4)	In 500 ml of bi-distilled water, dissolve: **121.14 g** of **Trizma-Base** adjust **pH** to **7.4** using *HCl*, bring the solution to **1 L** with bi-distilled water, Store at 4 °C
Homogenization buffer:	This buffer needs to be prepared fresh the day before or on the day of experiment and must be free of protease and phosphatase inhibitor cocktails
225 mM D-Mannitol, 75 mM Sucrose, 30 mM Tris–HCl (pH 7.4) 0.1 mM EGTA 1 mM PMSF	In 250 ml bi-distilled water, dissolve: **12.30 g D-Mannitol**, **7.7 g Sucrose**, add **9 ml 1 M Tris-HCl pH 7.4** If necessary adjust **pH** to **7.4**, then bring the solution to a final volume of **300 ml** with bi-distilled water Store at 4 °C Immediately before use add: **60 µl** of **0.5 M EGTA pH 7.4** and **3 ml** of **PMSF**
Mitochondria resuspending buffer (MRB): 250 mM D-mannitol 5 mM HEPES (pH 7.4) 0.5 mM EGTA	This buffer needs to be prepared fresh the day before or on the day of experiment and must be free of protease and phosphatase inhibitor cocktails In 45 ml of bi-distilled water, dissolve: **2.28 g D-Mannitol**, add **500 µl** of **0.5 M HEPES pH 7.4**, if necessary adjust **pH** to **7.4**, then bring the solution to a final volume of **50 ml** with bi-distilled water Store at 4 °C Immediately before use add: **50 µl** of **0.5 M EGTA** (pH 7.4)
Percoll medium: 225 mM D-Mannitol 25 mM HEPES (pH 7.4) 1 mM EGTA 30% Percoll (vol/vol)	This buffer needs to be prepared fresh the day before or on the day of experiment and must be free of protease and phosphatase inhibitor cocktails In 30 ml of bi-distilled water, dissolve: **2.052 g D-Mannitol**,add 2.**5 ml** of **0.5 M HEPES pH 7.4**, if necessary adjust **pH** to **7.4**, then bring the solution to a final volume of **35 ml** with bi-distilled water Store at 4 °C Immediately before add: **100 µl** of **0.5 M EGTA** (pH 7.4) and **15 ml** of **Percoll**

Reagents (Vendor, cat. no.): D-Mannitol (Sigma–Aldrich, cat. no. 4125), Dulbecco's phosphate-buffered saline (D-PBS), liquid, without Ca^{2+} and Mg^{2+} (Invitrogen, cat. no. 70011036), Ethylene-bis(oxyethylenenitrilo)tetraacetic acid.
(EGTA) (Sigma–Aldrich, cat. no. E3889), HEPES (Sigma–Aldrich, cat. no H3375), percoll (Sigma–Aldrich, cat. no. P1644), phenylmethanesulfonyl fluoride (PMSF) (Sigma–Aldrich, cat. no. P7626), protease inhibitor cocktail (100×) (Sigma–Aldrich, cat. no. P8340), sodium fluoride (Sigma–Aldrich, cat. no. S7920), sodium orthovanadate (Sigma–Aldrich, cat. no. S6508), Sucrose (Merck, cat. no. 100892.9050), Trizma-Base (Sigma–Aldrich, cat. no. T1503).
Bold values were used to help the reader in the quick identification of volumes and weights required for the preparation of the different buffers when performing the protocol. Italic values were used for a quick identification of the reagents to use to adjust the pH.

proteins that are not protected by closed phospholipidic bilayers. Using the method illustrated in Fig. 2 (see Table 2 for reagent setup), we observed significant PK digestion of hexokinase I (HK-I) that is loosely bound to the OMM through the voltage-dependent anion channel 1 (VDAC1), but not of VDAC that is an integral membrane protein. Similar to HK-I, PTEN was almost completely degraded by PK treatment, indicating that it was mainly loosely bound to the OMM, and not localized within the mitochondria. A similar conclusion was reached by studying the localization of the longer form of PTEN in comparison to PTEN [36]. The authors observed that the mitochondrial localization of the longer form of PTEN was much more prominent, compared to PTEN, and sub-fractionation of mitochondria isolated from the mouse brain cortex confirmed that PTEN is not able to enter the organelle. However, the longer PTEN form was preferentially associated with the mitochondrial inner membrane and is less abundant in the outer membrane, suggesting that the extended N-terminal region endows a distinct cellular localization and function.

The subcellular fractionation protocol depicted in Fig. 1 can also be used to study changes in subcellular localization of proteins in cells exposed to various treatments, such as apoptosis induction. This allowed us to prove that in cells treated with Arachidonic Acid (ArA), an apoptotic stimulus that induces Ca^{2+} transfer from the ER to the mitochondria [52], PTEN accumulated in the ER fraction [15]. In cells undergoing apoptosis, the isolation of the pure mitochondrial fraction may be difficult because of the ongoing rupture of the organelles [44,53]. Nevertheless, it is noteworthy that in response to ArA we observed a remarkable increase of VDAC at

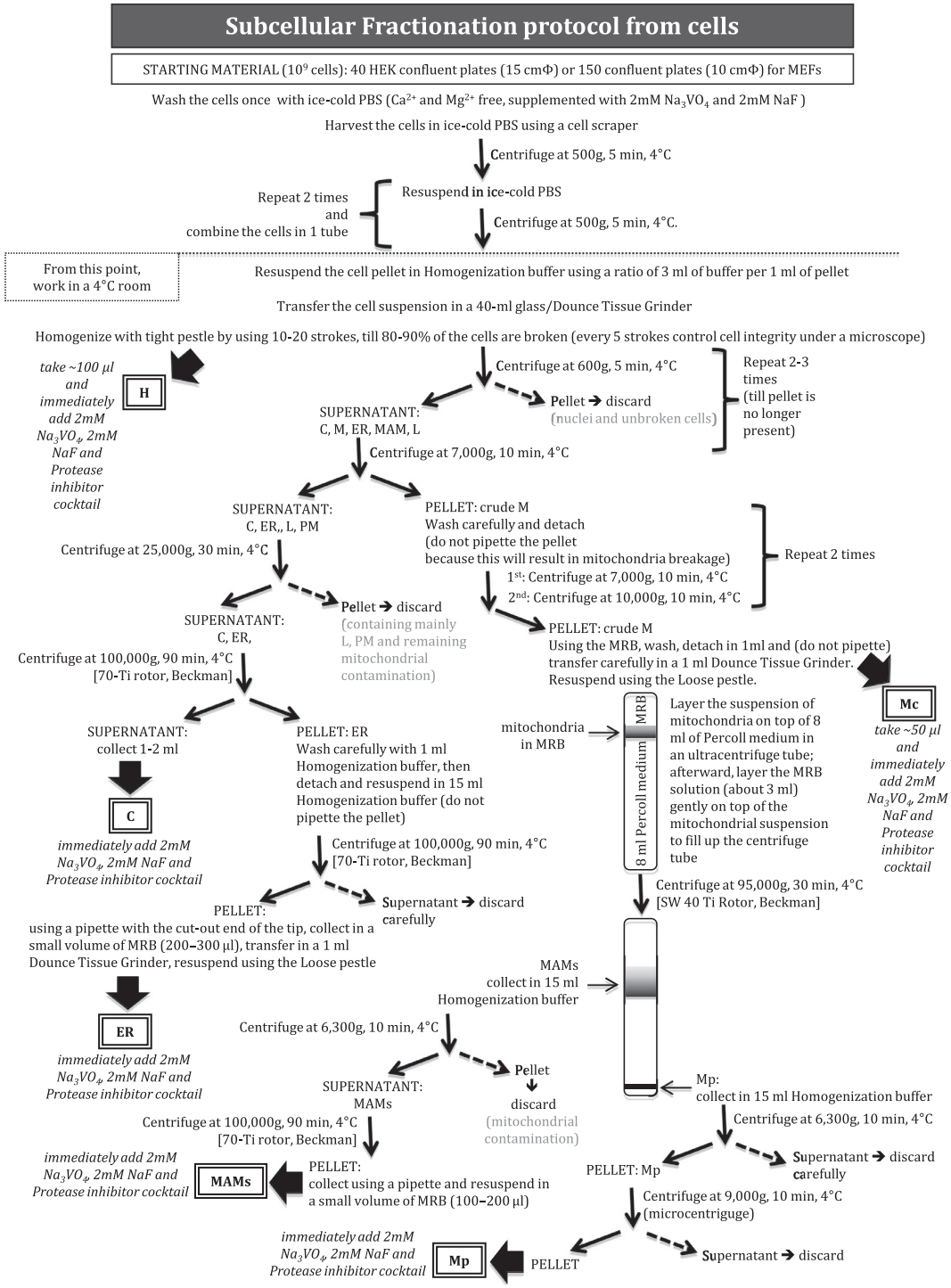

Fig. 1. Schematic steps of the subcellular fractionation protocol from cells. C, cytosol; ER: endoplasmic reticulum; H, homogenate; L: lysosomes; MAMs, mitochondria-associated membranes; Mc, crude mitochondria; Mp, pure mitochondria; PM, plasma membrane. Centrifugations were performed using a Beckman J2-21M/E refrigerated centrifuge, JA-20 Fixed Angle Rotor (tube: Beckman, cat. no. 363647). Ultracentrifugations were performed using a Beckman L8-70M ultracentrifuge, SW 40 Ti Rotor (tube: Beckman, cat. no. 344059), 70-Ti rotor (tube: Beckman, cat. no. 355618). For a detailed protocol see [51].

MAMs [15]. This is in agreement with previous studies demonstrating that under apoptosis-inducing conditions a narrowing of the ER-mitochondria associations occurs, and that this is an important step in the execution of some apoptotic mechanisms [54,55].

PTEN is regulated by multiple protein–protein interactions and the search for physiologically relevant protein substrates of PTEN continues. Thus, it is important to further investigate and understand the relevance of many of these interactions. To this end, we used the ER fraction (isolated as shown in Fig. 1) in co-immunoprecipitation (Co-IP) studies. Given the difference in composition between the homogenization buffers employed during subcellular fractionation (Table 1) and the common Co-IP-lysis buffers, we had to adjust the salt and detergent concentrations. Using the procedure described in Fig. 3, we were able to perform Co-IP experiments with proteins extracted from the ER fraction under basal conditions or after ArA treatment [15]. We found that

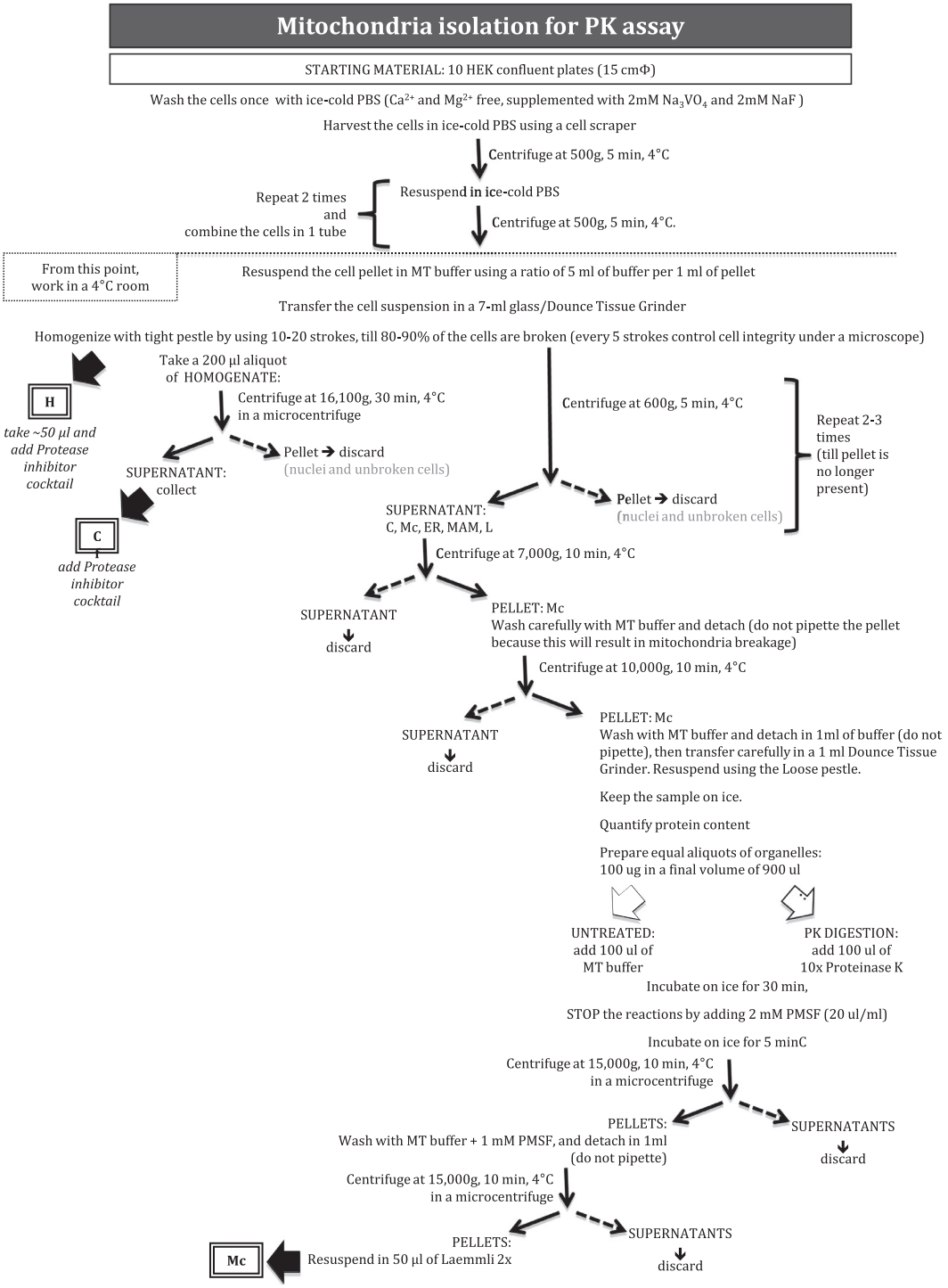

Fig. 2. Schematic steps of the Mitochondria isolation for PK assay protocol. Cf, cytosolic fraction; H, homogenate; Mc, crude mitochondria; PK, proteinase K. Centrifugations were performed using a Beckman J2-21M/E refrigerated centrifuge, JA-20 Fixed Angle Rotor (tube: Beckman, cat. no. 363647).

ER-localized PTEN co-immunoprecipitates with IP3R3. The increased ER localization of PTEN in ArA-treated cells results in a greater association between PTEN and IP3R3, and we also observed a concomitant reduction in both phosphorylated Akt ($pAkt^{Ser473}$) and phosphorylated IP3R3 present in the complex. These results suggest that when PTEN localizes to the ER, the Ca^{2+} flux through IP3R3 is strengthened by the inhibition of Akt activity.

Recently, we also established a protocol that allows the isolation of plasma membrane-associated membranes (PAMs), which are microdomains of the plasma membrane (PM) interacting with the ER and mitochondria (for a detailed protocol, see [56]). This procedure is another useful addition to the methods that can be employed to study the localization of PTEN, and in particular how it changes in response to different stimuli.

3. Cellular imaging methods

In addition to subcellular fractionation methods, there are a variety of cellular imaging methods that can be used to determine

Table 2
Setup of stock solutions and buffers to isolate mitochondria for PK assay. Catalog numbers of the reagents are provided at the bottom of the table.

Mitochondria isolation for PK assay stock solutions and buffers *Setup*	
0.1 M EGTA/Tris (pH 7.4)	In 90 ml of bi-distilled water, dissolve: **3.8 g** of **EGTA** adjust **pH** to **7.4** with *Tris powder*, bring the solution to **100 ml** with bi-distilled water, Store at 4 °C
0.1 M Tris–MOPS (pH 7.4)	In 900 ml of bi-distilled water, dissolve: **12.1 g** of **Trizma-Base** adjust **pH** to **7.4** using *MOPS powder*, bring the solution to **1 L** with bi-distilled water, Store at 4 °C
1 M sucrose	In 1 liter of bi-distilled water, dissolve: **342.3 g** of **Sucrose** mix well and prepare 25 ml aliquots, Store at −20 °C
Mitochondria buffer (MT):	This buffer needs to be prepared fresh on the day of experiment and must be free of protease and phosphatase inhibitor cocktails
10 mM Tris/MOPS (pH 7.4) 250 mM sucrose 0.1 mM EGTA/Tris	Add: **10 ml** of **0.1 M Tris–MOPS** and **100 µl** of **0.1 M EGTA/Tris** to **25 ml** of **1 M sucrose** Bring the volume to **100 ml** with distilled water, Adjust **pH** to **7.4** using *Tris* or *MOPS* powder, Store at 4 °C
10× proteinase K (PK)	This buffer needs to be prepared fresh immediately before use. In 10 ml of MT buffer, dissolve: **10 mg** of **proteinase K** Store on ice

Reagents (Vendor, cat. no.): Dulbecco's phosphate-buffered saline (D-PBS), liquid, without Ca^{2+} and Mg^{2+} (Invitrogen, cat. no 70011036), ethylene-bis(oxyethylenenitrilo)tetraacetic acid (EGTA) (Sigma–Aldrich, cat. no E3889), MOPS (Sigma–Aldrich, cat. no. M1254), Phenylmethanesulfonyl fluoride (PMSF) (Sigma–Aldrich, cat. no. P7626), Protease inhibitor cocktail (100×) (Sigma–Aldrich, cat. no. P8340), proteinase K from *Tritirachium album* (Sigma–Aldrich, cat. no. P2308), sucrose (Merck, cat. no. 100892.9050), Trizma-base (Sigma–Aldrich, cat. no. T1503).
Bold values were used to help the reader in the quick identification of volumes and weights required for the preparation of the different buffers when performing the protocol. Italic values were used for a quick identification of the reagents to use to adjust the pH.

the subcellular localization of proteins. Immunostaining can be used to compare the localization of a protein of interest against known markers. Another widespread approach that has been used to study PTEN localization is the generation of fusion proteins tagged with GFP or its derivatives. In-frame fusion of the GFP and the PTEN cDNAs makes it possible to examine function as well as fate of the resulting chimera in living cells. The subcellular localization of the fusion protein, if not immediately apparent, can then be determined by comparisons to that of various organelles or subcellular structures targeted by fluorescent fusion proteins with different spectral properties, or by direct comparison with fluorescent dyes.

Because PTEN regulates the PI3K–AKT pathway, initial studies were focused on how PTEN is able to gain membrane localization in order to access its substrates. Using a laser scanning confocal microscope, immunostaining of FLAG-PTEN was observed in discrete membranous regions at sites of cellular projections in MDCK kidney epithelial cells [57]. Iijima et al. used fluorescence microscopy to study the binding of PTEN to the PM in living cells. Full-length PTEN or mutant PTEN variants were fused to GFP at the C-terminus (PTEN-GFP) and expressed in *Dictyostelium discoideum pten*$^-$ cells. This approach was used to demonstrate that the PIP2 binding motif at the N-terminus of PTEN is important for both its localization and regulation of activity, and to study how chemoattractant stimuli alter PTEN or mutant PTEN localization [10,58]. Later, Vazquez et al. developed a single-molecule imaging of functionally active PTEN-yellow fluorescent protein (YFP) to study why PTEN was found to translocate to the PM only in certain cell lineages and under specific conditions. The low levels of PTEN on the membrane, coupled to the limitations epi-fluorescence microscopy (EPI-FM), made it difficult to detect PTEN. Therefore, they used single-molecule Total Internal Reflection Fluorescence Microscopy (TIRFM) in living cells to reveal that PTEN-YFP associates stably, albeit transiently (approximately 150 ms), with the PM [9].

Immunofluorescence (IF) and confocal microscopy were recently used to demonstrate that SUMOylation facilitates PTEN association with the PM. Subcellular localizations of PTEN and PIP3 were monitor in MEFs wild type or lacking the SUMO-specific protease 1 (SENP1), which is the main de-SUMOylation enzyme for SUMO1-conjugated substrates. The quantitative analysis of PTEN and PIP3 membrane-to-cytosol ratios revealed and higher PTEN membrane localization in *SENP1*-null MEFs compared to WT MEFs; conversely, the membrane-to-cytosol ratio of PIP3 was markedly decreased in MEFs lacking SENP1 [23].

Several other studies demonstrated that nuclear PTEN is essential for tumor suppression. Nuclear localization of PTEN was observed for the first time in PC12 cells after immunostaining for endogenous PTEN or recombinant HA-tagged PTEN [47]. In differentiating PC12 cells, PTEN was most evident as speckles in the nucleus, with only a faint diffuse staining in the cytoplasm. More mature PC12 cells, however, showed strong staining in both the cytoplasm and nucleus. As anti-PTEN antibodies do not always faithfully report on subcellular distributions of PTEN, studies of PTEN localization based on IF must always take into account PTEN antibody specificity. A panel of commercially available anti-PTEN antibodies was tested in *Pten*-WT and *Pten*-null MEFs, and also in PTEN WT (U2OS and HCT116) or PTEN-null (PC3) human cancer cell lines [29].

Centromeric localization of PTEN was also detected by using a double IF procedure [30]. *Pten*-WT and *Pten*-null MEFs were fixed and incubated with either an anti-PTEN monoclonal antibody

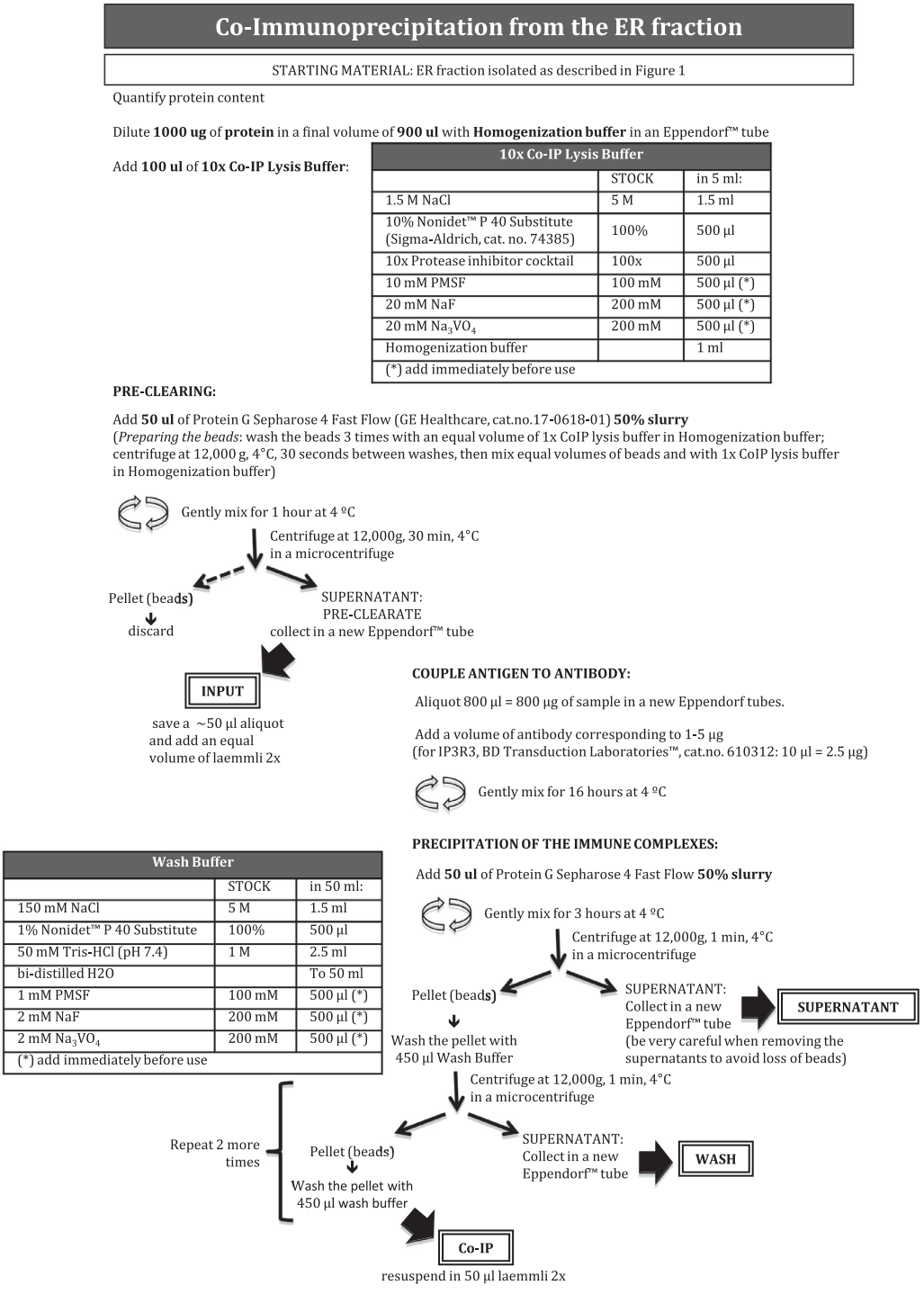

Fig. 3. Schematic protocol to co-immunoprecipitate proteins from the ER fraction.

(Santa Cruz), or a homemade anti-full-length PTEN polyclonal antibody, together with the human CREST autoimmune sera against centromere/kinetochore antigens (ImmunoVision). Image analysis using a laser-scanning confocal microscope revealed an overlapping spatial relationship between the PTEN signal (in green) and the centromere (in red) as a signal of discrete yellow speckles, indicating that a significant portion of nuclear PTEN colocalizes with centromeres in *Pten*-WT MEFs. The PTEN signal was undetectable in *Pten*-null MEFs, confirming the specificity of the PTEN antibody.

Recently, IF analysis also led to the identification of nucleolus-localized PTEN in HeLa and COS-1 cells [13]. This was validated by co-staining the same cells for PTEN and Nucleolin (a nucleolar marker). Non-specificity of the PTEN antibody was excluded by using several controls, including the PTEN-negative PC3 and LNCaP cell lines, or HeLa cells in which PTEN had been silenced.

PTEN monoubiquitinylation by the E3-ligase NEDD4-1 allows PTEN to accumulate in the nucleus [11], whereas PTEN deubiquitinylation HAUSP favors PTEN accumulation in the cytoplasm [29]. In IF studies of *PML*-null MEFs revealing a significantly increased fraction of cytoplasmic PTEN was the first observation leading to the identification of the PML–DAXX (death domain-associated protein)–HAUSP molecular network in regulating deubiquitinylation-

Four Colors Immunofluorescence

STARTING MATERIAL: cells grown on 24mm round glass coverslips (or on commercially available incubation chambers)

A. CELL PREPARATION AND TRANSFECTION FOR MITOCHONDRIA LABELING (*Red*):
A-1. *Cell growth.*
Preparation of coverslips for HEK-293 (and other non-adherent cell lines): place coverslips in a multi-well plate and coat them with an excess of 1x poly-L-lysine (Sigma-Aldrich, cat. no. P4707) in PBS for 1 hr at room temperature, than wash 3 times with sterile ultrapure H2O and allow coverslips to dry completely (for at least 1 hour before seeding the cells).
Seed the cells on round glass coverslips (diameter, 24 mm) and allow them to grow until ~50% confluent. After cell seeding, wait at least 48 h if you are using HEK-293T (24 h are usually enough for the majority of cell lines)
A-2. *Transfection.*
When the cells have reached 40–50% confluence, transfect them with 2-3 μg of vector encoding mtDsRED per coverslip (depending on the desired transfection method it is possible to use also a lower amount of DNA; 2-3 μg are suggested if you are using a standard calcium phosphate procedure). After transfection, wait 36–48 h.

B. NUCLEI STAINING (*Blue*):
B-1. Remove medium and wash 3 times with 2 ml PBS per well.
B-2. Stain nuclei with **0.25 μg/ml Hoechst 33342** (life technologies, cat. no. H3570) in PBS, for 10 min at 37°C, in the dark. From now on minimize exposure to light.
B-3. Remove the staining solution and wash 3 times with 2 ml PBS per well.

C. PARAFORMALDEHYDE FIXATION:
C-1. Add 2 ml per well **of 4% paraformaldehyde in PBS** (freshly prepared in a fume hood) and incubate for 15 minutes at 37°C.
C-2. Wash monolayer in PBS, three times for 5 minutes with gentle shaking, to remove residual paraformaldehyde.

D. PERMEABILIZATION:
D-1. Add 2 ml per well of PBS containing **0.1% Triton X-100** (Sigma-Aldrich, cat. no. T8787) and incubate for 10 minutes at RT with gentle shaking.
D-2. Wash 2 times with 2 ml PBS per well.

E. BLOCKING:
Incubate with 2 ml per well **of Blocking Buffer (1% BSA in PBS)** for 20 minutes at RT, to block unspecific binding of the antibodies.

F. PRIMARY ANTIBODIES:
F-1. Remove the blocking buffer by holding each coverslip on its edge with forceps and draining it onto a sheet of fiber-free paper.
F-2. Dilute the mixture of the 2 primary antibodies in blocking buffer:
- Mouse monoclonal to **PTEN (A2B1) (Santa Cruz, cat. no. sc-7974), 1:50**
- Rabbit polyclonal to **PDI – ER marker (1 : 100, Abcam, cat. no. ab3672), 1:100**
Antibody incubation require a small volume. Do it in a humidified chamber made from a 15 cm petri dish with PBS-soaked filter paper covered by a layer of parafilm.
Place a 50 μl drop of the primary antibodies solution on the parafilm, and turn cell-side down the coverslip on the drop. Incubate overnight at 4°C in the humidified chamber.

G. WASHES:
Add 2 ml per well of **0.1% Triton X-100** and carefully turn the coverslips cell-side up; wash three times for 5 minutes with gentle shaking.

H. SECONDARY ANTIBODIES (*Green & Far Red*):
Incubate with the mixture of 2 secondary antibodies which are raised in different species (with two different fluorochromes, i.e. Far Red-conjugated against rabbit and FITC-conjugated against mouse) in blocking buffer:
- Alexa Fluor **488** goat anti-mouse (life technologies, cat. no. A-11001), 1:1000
- Alexa Fluor **633** Goat Anti-Rabbit (life technologies, cat. no. A-21070), 1:1000
Place coverslips cells-side-up in in the humidified chamber, add 200 μl of the mixture of the secondary antibodies solution, and incubate for 1 hour at room temperature in the dark.

I. WASHES:
I-1. Remove the secondary antibody by blotting the edge of each coverslip on fiber-free paper and wash three times in 2 ml **0.1% Triton X-100** per well for 5 min each, with gentle shaking in the dark.
I-2. Remove the 0.1% Triton X-100 and leave the coverslip in **PBS**.

J. MOUNTING:
J-1. Invert each coverslip onto a slide containing a drop of mounting medium (**ProLong Gold antifade reagent**; life technologies, cat. no. P36934).
J-2. The day after, seal the edges of each coverslip with regular transparent **nail polish** to prevent drying and movement under microscope.
J-3. Store in dark at -20°C or 4°C until image acquisition.

Fig. 4. Four colors immunofluorescence protocol. Cells can be grown directly on coverslips. Use thickness 1.5 mm coverslips, as most microscope objectives are designed to work optimally with these. Coverslips must be sterilized and then placed in a multi-well plate: 18 mm coverslips in a 12 well plate, 12–13 mm coverslips in a 24-well plate, or 24 mm coverslips in a 6-well plate. Use forceps with a fine tip for handling the coverslips. In [15] images were acquired on an Axiovert 220 M microscope equipped with a ×100 oil immersion Plan-Neofluar objective (NA 1.3, from Carl Zeiss, Jena, Germany) and a CoolSnap HQ CCD camera. Each field was acquired over 26 z-planes spaced by 0.4 μm. Image sampling was below resolution limit and calculated according to the Nyquist calculator (available at http://www.svi.nl/NyquistCalculator). After acquisition, z-stacks were deconvoluted with the 'Parallel Iterative Deconvolution' plugin of the open source Fiji software (freely available at http://fiji.sc/). Controls to be included: (i) incubation with secondary antibody only (to determine non-specific staining of the secondary antibody), (ii) non-immune serum or isotype Ig (matching the primary antibody, to determine non-specific staining of the primary antibody), (iii) also a non-processed sample to control autofluorescence may be needed.

dependent PTEN subcellular compartmentalization. The overlay of PTEN and PML staining also showed that PTEN co-localized to nuclear bodies in *PML*-WT but not *PML*-null MEFs [29]. In dysplastic intestinal polyps from Cowden syndrome patient colon sample slides, stained for PTEN using the monoclonal 6H2.1 (Cascade) or the polyclonal Ab-2 (Nemoarkers) antibodies, it was observed that the cancer-associated lysine mutant of PTEN(K289E) (which retains catalytic activity) was excluded from the nucleus [11].

PTEN was excluded from the nuclei of epithelial cells, but remarkably, interstitial lymphocytes (which retain both WT and K289E mutant proteins) retained nuclear PTEN staining, serving as internal control for the staining procedure. To test mutant PTEN localization, the authors also generated GFP fusion chimeras of WT PTEN and PTEN(K289E). Within 10–12 h after transient transfection in PTEN-deficient prostate cancer cells (PC3), WT PTEN efficiently equilibrated between the nucleus and cytoplasm, while the PTEN(K289E) mutant predominantly showed cytoplasmic accumulation in most cells. To quantitatively test the nuclear and cytoplasmic accumulation rates of the PTEN mutant, the authors used FRAP. This technique produces distinguishable cytoplasmic and nuclear PTEN populations by bleaching GFP fluorescence in either the cell nucleus or cytoplasm. Then, the authors used time-lapse florescence microscopy to measure the compartmental equilibration, which occurs via nuclear import and export. They found that WT PTEN fluorescence re-accumulated inside the nucleus, reaching equilibrium by approximately 15 min post-nuclear bleaching. In contrast, the PTEN(K289E) mutant showed a clearly reduced nuclear accumulation and no equilibration within the same period. Calculation of the nuclear accumulation rates revealed an 18-fold reduction in nuclear net import of the K289E mutant [11].

In an analogous way, nuclear FRAP of cherry-PTEN was used also to demonstrate that nuclear import of PTEN is accelerated by Ndfip1, an adaptor for NEDD4-mediated ubiquitination [33]. Co-overexpression of GFP-Ndfip1 strongly accelerated recovery of nuclear cherry-PTEN fluorescence after nuclear bleaching (from >800 s to <500 s), with an apparent import rate greater than four-fold higher than what was observed in GFP-expressing cells. The authors also provided the first *in vivo* example of an acute stimulus that can regulate nuclear trafficking of PTEN: confocal microscopy of a brain section in the non-ischemic hemisphere of WT mice showed low levels of basal Ndfip1 expression together with cytoplasmic PTEN in these neurons, while in the ischemic cortex of WT mice relocalization of PTEN to the nucleus was strongly correlated with neurons up-regulating Ndfip1. Since Ndfip1 induction protects neurons from ischemic death, also nuclear PTEN import appears to promote neuronal survival following cerebral ischemia.

More recent studies have also found PTEN localized to the mitochondria, the ER, and the MAMs. The first observation of PTEN accumulation in mitochondria originated from experiments designed to study the molecular mechanism of PTEN in neuronal apoptosis [14]. The authors evaluated the intracellular distribution of PTEN in primary rat hippocampal cultures that were treated with 100 nM STS or the vehicle control. Cells were treated with the apoptotic stimulus STS, fixed and immunostained with a monoclonal anti-PTEN antibody (1:100, Cell Signaling Technology), and analyzed using a confocal laser scanning microscope. Immunoreactivity of PTEN was detected in both the cytoplasm and nucleus under control conditions. Between 2 h and 8 h after STS treatment the immunoreactivity of PTEN scattered as dots in the cytoplasm, but this expression pattern was no longer observed at 24 h when cells were severely damaged. No detectable signal was observed in negative controls, in which cells were incubated with the blocking buffer without the primary antibody. To confirm that this alteration in the subcellular localization of PTEN was caused by its

Live Colocalization

STARTING MATERIAL: cells grown on 24mm round glass coverslips

A. CELL PREPARATION, TRANSFECTION WITH GFP-PTEN (*Green*) AND TRANSDUCTION FOR ER LABELING (*Red*):
A-1. *Cell growth.*
For coverslip preparation and HEK-293 seeding: see Figure 4.
A-2. *Transfection.*
When the cells have reached 40–50% confluence, transfect them with 2-3 µg of vector encoding **GFP-PTEN** (or **GFP** as control) per coverslip. Wait 24 h.
A-3. *Transduction.*
Cells should be less than 70% confluent at the moment of transduction with **CellLight® ER-RFP, BacMam 2.0** (life technologies, cat. no. C10591). One hour before transduction, replace the media and leave the cells in 1.5 ml per well. Calculate the appropriate volume of CellLight® reagent based on cell number.

Volume of CellLight® Reagent (mL) = (number of cells * desired PPC)/($1*10^8$ CellLight® particles/mL)

We considered a PCC = 10.

Mix the reagent and add the calculated volume to each well, rock gently the plate and return it to the incubator.
Wait 16-24 hours.

B.TIME-LAPS RECORDING OF GFP-PTEN DYNAMYCS DURING APOPTOTIC STIMULATION:
In [15] images were acquired using a **Nikon Swept Field Confocal** equipped with CFI Plan Apo VC60XH objective (numerical aperture, 1.4) (Nikon Instruments, Melville, NY, USA) and an Andor DU885 electron multiplying charge coupled device (EM-CCD) camera (Andor Technology Ltd, Belfast, Northern Ireland), the overall image sampling was below the resolution limit (X and Y pixel size: 133 nm).

B-1. *Coverslip set-up.* Wash 3 times with Krebs-Ringer buffer (KRB: 135mM NaCl, 5mM KCl, 1mM $MgSO_4$, 0.4mM KH_2PO_4, 5.5mM glucose, 20mM HEPES, pH 7.4) supplemented with 1mM $CaCl_2$, then place the coverslip in an open Leyden chamber on an incubated microscope stage with controlled temperature, CO_2 and humidity.

B-2. *Time-Laps recording:*
-Acquire **basal** fluorescence images for **5 min**,
-stimulate with ArA (80 µM final in KRB),
-acquire fluorescence images every **3 minutes for 30 minutes**,
-then acquire images every **10 minutes for 1** further **hour** (to avoid bleaching of the fluorophores).

C. QUANTITATIVE COLOCALIZATION ANALYSIS:
Analyze acquired images using the open source software **Fiji** (http://fiji.sc/Fiji):
-correct images for spectral bleedthrough using the **Spectral Unmixing plugin** (available at http://rsb.info.nih.gov/ij/plugins/spectral-unmixing.html).
-for every cell positive for coexpression of GFP-PTEN (or GFP) and ER-RFP, calculate the Manders' overlap coefficient using the **JACOP plugin.41** (http://rsbweb.nih.gov/ij/plugins/track/jacop.html).

Fig. 5. Live colocalization analysis. Calculate Manders' overlap coefficients for at least three independent experiments and consider as translocated those cells that show a significant increase at the end of the experiment compared with the beginning.

translocation to the mitochondria during the apoptotic process, the cells were double-labeled with PTEN and MitoTracker Orange, a cell membrane-permeable dye that can selectively label mitochondria in living cells. STS-induced punctate immunoreactivity of PTEN was colocalized with the mitochondrial marker, indicating an accumulation of PTEN in the mitochondria. In double labeling IF, the authors also observed a colocalization of PTEN with Bax after STS challenge, suggesting that PTEN and Bax were both translocated to the mitochondria. Of note, Bax was located in the cytosol under control conditions, whereas PTEN was located in both the cytosol and nucleus.

In transfected *Pten*-null MEFs, MitoTracker staining was also used to label mitochondria and evaluate potential colocalization of GFP-tagged PTEN, or its longer form PTEN-L, with the mitochondria [36]. Overlayed, merged images of GFP and MitoTracker collected using a confocal fluorescence microscope showed a substantial colocalization of PTEN-L with the mitochondria, whereas mitochondrial colocalization of PTEN was less prominent. To further examine the subcellular localization of PTEN-L and to compare it with that of PTEN, the authors also employed a protease protection assay. PTEN-null MEFs transfected with GFP-tagged PTEN-L or PTEN were subjected to consecutive digestion with digitonin (80 μM, 60 s: cytoplasmic membrane permeabilization) and trypsin (0.5 mM, 2 min: removal of cytosolic-exposed terminals of organelle-associated proteins). They observed two distinctly different patterns: (i) PTEN was ubiquitously distributed in both the cytoplasm and the nucleus prior to digitonin treatment, and the treatment eliminated the majority of the cytoplasmic PTEN signal; and (ii) PTEN-L displayed predominantly cytoplasmic localization before digitonin treatment, and the signal was partially retained after the treatment. Further trypsin digestion removed all GFP-tagged PTEN signals, but did not affect digitonin-retained PTEN-L signals. These results confirmed that PTEN-L can be cytosolic or associated with cytoplasmic organelles, such as the mitochondria, whereas PTEN is mainly cytosolic or nuclear.

We also used a four-color IF in order to simultaneously analyze the staining of PTEN (using PTEN (A2B1) antibody, 1:50, Santa Cruz) and markers for the nucleus (Hoechst), mitochondria (transfection with mtDsRED), and ER (PDI antibody, 1:100, Abcam), in HEK-293T cells [15]. To our knowledge, this was the first time that this approach was used for PTEN (the specific procedure we used is shown in Fig. 4). Merged images revealed a typically diffuse, punctate staining pattern of PTEN that partially colocalized with the ER, the mitochondrial network and the nucleus.

We also used a GFP-PTEN chimera [11] to follow PTEN subcellular localization and changes occurring during Ca^{2+}-mediated apoptosis. Our goal was to gain insights into the role of PTEN localization at the ER and sensitivity to apoptosis, in response to increasing Ca^{2+} release via IP3Rs. We co-transfected HEK-293 cells with GFP-PTEN, and CellLight ER-Red Fluorescent Protein (RFP) BacMam 2.0 (Life Technologies) [59], which encodes RFP fused to the ER signal sequence of calreticulin and KDEL (an ER retention signal), providing an easy method for the labeling of the ER with RFP in live cells. After 90 min of apoptotic challenge, we observed a substantial increase in GFP-PTEN colocalization with the ER marker ER-RFP, indicating a strong enrichment of PTEN to the ER in cells undergoing apoptosis. In contrast, no significant differences were observed in control GFP-transfected cells before or after treatment. We quantified the extent of signal overlap between PTEN and the ER by calculating the Manders' coefficients (green and red), which measure colocalization as the fraction of each probe that is colocalized with the other. Manders' coefficients are described by an equation that is implemented in image analysis software packages, such as Colocalizer Pro, Image-Pro, Imaris, and Volocity and can be implemented in ImageJ via the JACoP plugin. Manders' coefficients analysis is also more appropriate for three-dimensional analysis of colocalization, which is required for studies in which probe colocalization varies spatially within a cell, and does not require the delineation of the region-of-interest [60]. A summary of this experiment is provided in Fig. 5.

4. Selective subcellular targeting of PTEN to study its functions in different cellular compartment

Targeting is a powerful and commonly used approach for studying the functions and localization of proteins in eukaryotic cells. Advances in molecular biology techniques have made it possible to modify the subcellular localization of a protein by the addition of specific targeting sequences. Thus, protein chimaeras endowed with a defined intracellular localization can be constructed.

Table 3
Description of the compartment-specific PTEN chimeras available.

Targeting PTEN to different organelles and cell compartments		
Acronym	Intracellular localization	Targeting strategy
GFP-PTEN-NLS^{SV-40}	*Nucleus*	GFP-PTEN-NLS [11] was constructed by cloning the triple NLS (from SV40) of pEYFP-Nuc (Clontech, #6905-1) into the 3-prime end of GFP-PTEN (produced by subcloning PTEN from pCDNA3 into pEGFP-C2 (Clontech, #6083-1))
GFP-PTEN-NES^{PKI}	*Cytoplasm*	GFP-PTEN-NES^{PKI} was constructed by cloning synthetic oligos corresponding to the NES sequence of the PKI protein (-LALKLAGL-) to the 3-prime end of GFP-PTEN [11]
snap25-PTEN	*Plasma membrane (inner surface)*	SNAP-25 protein is synthesized on free ribosomes and recruited to the inner surface of the plasma membrane after the palmitoylation of specific cysteine residues SNAP-25 coding sequence was amplified from snap25-aequorin and then subcloned (KpnI/BamHI) to the N-terminus of human PTEN cloned (EcoRI/EcoRI) in pcDNA3.1, to generate snap25-PTEN [15]
AKAP-PTEN	*Outer mitochondrial membrane (cytoplasmic surface)*	A kinase anchoring protein 1 (AKAP1) is a scaffold protein that recruits protein kinase A (PKA) and other signaling proteins, as well as RNA, to the outer mitochondrial membrane (OMM) AKAP-PTEN was constructed by fusing the N-terminal mitochondrial localization sequence of the mouse AKAP1 protein (from GenBank/EMBL/DDBJ under accession no. V84389; residues 34–63; amplified as BglII–HindIII from OMM-IP3R-LBD and then subcloned) to the N-terminus of human PTEN cloned (EcoRI/EcoRI) in pcDNA3.1 [15]
ER-PTEN ER-PTEN(C124S) ER-PTEN(G129E)	*Endoplasmic reticulum (cytoplasmic surface)*	UBC6, native to *Saccharomyces cerevisiae*, is a 250-amino acid ER resident membrane-anchored ubiquitin-conjugating enzyme, which has no known ER retention/retrieval signal PTEN was localized to the cytoplasmic surface of the ER membrane (ER-PTEN) by subcloning (KpnI/BamHI) a sequence from UBC6 (-MVYIGIAIFLFLVGLFMK-) [50] to the N-terminus of human PTEN cloned (EcoRI/EcoRI) in pcDNA3.1 [15] ER-PTEN(C124S) and ER-PTEN(G129E) were obtained by substituting the human PTEN coding sequence of ER-PTEN with those of human PTEN(C124S) or (G129E) mutants [32] (subcloned EcoRI/XhoI) [15]

We used this strategy to target PTEN to different organelles and cell compartments, thus generating novel tools for investigating the spatial complexity of PTEN functions. Previously, PTEN chimeras were generated by forced localization to either the nucleus (PTEN-NLS^{SV-40}) by fusion to a NLS, or to the cytoplasm (PTEN-NES^{PKI}) by fusion with a nuclear export signal (NES) [11]. In addition, we generated specific chimeric proteins that targeted the entire PTEN protein exclusively to the PM (snap25-PTEN), to the OMM (AKAP-PTEN) or to the cytoplasmic surface of the ER membrane (ER-PTEN) [15]. Details on the construction of the different chimeras are described in Table 3. In all cases, correct intracellular localization of the PTEN-chimeras has been verified through IF, using antibodies against PTEN and specific markers for the various intracellular compartments.

Co-transfection of these chimeras, together with mitochondrial targeted aequorin [61], allowed us to analyze whether a particular subcellular localization of PTEN could differentially affect mitochondrial Ca^{2+} homeostasis. We demonstrated that specific targeting of PTEN to the ER is sufficient to enhance ER-to-mitochondria Ca^{2+} transfer and sensitivity to apoptosis [62].

We also dissected the precise contribution of PTEN's lipid and protein phosphatase activities in the regulation of Ca^{2+} signaling and apoptosis, by generating ER-targeted chimeras of the PTEN(C124S) mutant [2], which lacks both lipid and protein phosphatase activities (ER-PTEN(C124S)), and of the PTEN(G129E) mutant [4], which displays a minimal lipid phosphatase activity while retaining full protein phosphatase activity (ER-PTEN(G129E)). Using this approach, we demonstrated that the ER pool of PTEN counteracts Akt activation specifically at the ER, and can thus inhibit the Akt-mediated phosphorylation of IP3R3 that protects from Ca^{2+}-mediated apoptosis [43]. We concluded that the ability of ER-localized PTEN to regulate Ca^{2+} release from the ER specifically relies on its protein phosphatase activity [15].

5. Concluding remarks

The past few years have seen the development and acceptance of the notion that PTEN is far more than a cytosolic resident protein capable of interacting with the PM and acting as a lipid phosphatase to keep the levels of PIP3 low. PTEN has a full set of additional functions in almost every subcellular compartment, and possesses functions beyond its phosphatase activity. This evidence not only urged us to reconsider the conventional wisdom about PTEN but also raised a number of new and exciting questions about the unique role of PTEN in a specific compartment, the mechanisms regulating the pleiotropic functions of PTEN, and the methods best suited to address these questions. In this review, we have summarized the main biochemical, imaging and molecular biology methods that have been employed to-date to piece together this complicated picture. Adding new pieces to this puzzle will offer new insights into the cellular landscape of PTEN activity and function, aiding in the clinical management and treatment of human cancers and neurological disorders in which PTEN is lost or mutated.

Acknowledgements

This study was supported by: the Italian Association for Cancer Research (AIRC), Telethon (GGP11139B), the Italian Ministry of Health, the Italian Ministry of Education, University and Research (COFIN, FIRB, and Futuro in Ricerca) and local funds from the University of Ferrara to Paolo Pinton.

References

[1] N. Dey et al., Cancer Res. 68 (6) (2008) 1862–1871.
[2] T. Maehama, J.E. Dixon, J. Biol. Chem. 273 (22) (1998) 13375–13378.
[3] V. Stambolic et al., Cell 95 (1) (1998) 29–39.
[4] M.P. Myers et al., Proc. Natl. Acad. Sci. U.S.A. 95 (23) (1998) 13513–13518.
[5] M.C. Hollander, G.M. Blumenthal, P.A. Dennis, Nat. Rev. Cancer 11 (4) (2011) 289–301.
[6] C. Eng, Hum. Mutat. 22 (3) (2003) 183–198.
[7] A. Di Cristofano et al., Nat. Genet. 19 (4) (1998) 348–355.
[8] M.S. Song, L. Salmena, P.P. Pandolfi, Nat. Rev. Mol. Cell Biol. 13 (5) (2012) 283–296.
[9] F. Vazquez et al., Proc. Natl. Acad. Sci. U.S.A. 103 (10) (2006) 3633–3638.
[10] M. Iijima et al., J. Biol. Chem. 279 (16) (2004) 16606–16613.
[11] L.C. Trotman et al., Cell 128 (1) (2007) 141–156.
[12] C. Bassi et al., Science 341 (6144) (2013) 395–399.
[13] P. Li et al., Mol. Biol. Rep. 41 (10) (2014) 6383–6390.
[14] Y. Zhu et al., Apoptosis 11 (2) (2006) 197–207.
[15] A. Bononi et al., Cell Death Differ. 20 (12) (2013) 1631–1643.
[16] U. Putz et al., Sci. Signal. 5 (243) (2012) ra70.
[17] B.D. Hopkins et al., Science 341 (6144) (2013) 399–402.
[18] S.M. Walker et al., Biochem. J. 379 (Pt 2) (2004) 301–307.
[19] R.E. Redfern et al., Biochemistry 47 (7) (2008) 2162–2171.
[20] J.O. Lee et al., Cell 99 (3) (1999) 323–334.
[21] F. Vazquez et al., Mol. Cell. Biol. 20 (14) (2000) 5010–5018.
[22] F. Vazquez et al., J. Biol. Chem. 276 (52) (2001) 48627–48630.
[23] J. Huang et al., Nat. Commun. 3 (2012) 911.
[24] O. Gimm et al., Am. J. Pathol. 156 (5) (2000) 1693–1700.
[25] F. Liu et al., J. Cell. Biochem. 96 (2) (2005) 221–234.
[26] J.H. Chung, M.E. Ginn-Pease, C. Eng, Cancer Res. 65 (10) (2005) 4108–4116.
[27] G. Denning et al., Oncogene 26 (27) (2007) 3930–3940.
[28] A. Gil et al., Mol. Biol. Cell 17 (9) (2006) 4002–4013.
[29] M.S. Song et al., Nature 455 (7214) (2008) 813–817.
[30] W.H. Shen et al., Cell 128 (1) (2007) 157–170.
[31] S.M. Planchon, K.A. Waite, C. Eng, J. Cell Sci. 121 (Pt 3) (2008) 249–253.
[32] M.S. Song et al., Cell 144 (2) (2011) 187–199.
[33] J. Howitt et al., J. Cell Biol. 196 (1) (2012) 29–36.
[34] Y. Lindsay et al., J. Cell Sci. 119 (Pt 24) (2006) 5160–5168.
[35] L. Zu et al., Am. J. Physiol. Heart Circ. Physiol. 300 (6) (2011) H2177–H2186.
[36] H. Liang et al., Cell Metab. 19 (5) (2014) 836–848.
[37] S. Marchi, S. Patergnani, P. Pinton, Biochim. Biophys. Acta 1837 (4) (2014) 461–469.
[38] S. Patergnani et al., Cell Commun. Signal. 9 (2011) 19.
[39] C. Giorgi et al., Cell Calcium 52 (1) (2012) 36–43.
[40] T. Szado et al., Proc. Natl. Acad. Sci. U.S.A. 105 (7) (2008) 2427–2432.
[41] S. Marchi et al., Biochem. Biophys. Res. Commun. 375 (4) (2008) 501–505.
[42] S. Marchi et al., Cell Death Dis. 3 (2012) e304.
[43] C. Giorgi et al., Science 330 (6008) (2010) 1247–1251.
[44] M. Bonora et al., Cell Cycle 12 (4) (2013) 674–683.
[45] R. Pulido et al., Sci. Signal 7 (332) (2014) pe15.
[46] N.R. Leslie et al., Biochem. J. 357 (Pt 2) (2001) 427–435.
[47] M.B. Lachyankar et al., J. Neurosci. 20 (4) (2000) 1404–1413.
[48] Y. Ohmori, R.D. Schreiber, T.A. Hamilton, J. Biol. Chem. 272 (23) (1997) 14899–14907.
[49] H. Busch et al., Exp. Cell Res. 24 (Suppl. 9) (1963) 150–163.
[50] C. Frezza, S. Cipolat, L. Scorrano, Nat. Protoc. 2 (2) (2007) 287–295.
[51] M.R. Wieckowski et al., Nat. Protoc. 4 (11) (2009) 1582–1590.
[52] A. Bononi et al., Adv. Exp. Med. Biol. 740 (2012) 411–437.
[53] M. Bonora et al., Oncogene (2014).
[54] G. Csordas et al., J. Cell Biol. 174 (7) (2006) 915–921.
[55] D. De Stefani et al., Cell Death Differ. 19 (2) (2012) 267–273.
[56] J.M. Suski et al., Nat. Protoc. 9 (2) (2014) 312–322.
[57] X. Wu et al., Proc. Natl. Acad. Sci. U.S.A. 97 (8) (2000) 4233–4238.
[58] M. Iijima, P. Devreotes, Cell 109 (5) (2002) 599–610.
[59] T.A. Kost, J.P. Condreay, D.L. Jarvis, Nat. Biotechnol. 23 (5) (2005) 567–575.
[60] H. Persson et al., Acta Physiol. Scand. 134 (4) (1988) 565–566.
[61] M. Bonora et al., Nat. Protoc. 8 (11) (2013) 2105–2118.
[62] S. Marchi, P. Pinton, J. Physiol. 592 (Pt 5) (2014) 829–839.